SSRG International Journal of Electrical and Electronics Engineering
ISSN: 2348-8379/ https://doi.org/10.14445/23488379/IJEEE-V12I4P113

Volume 12 Issue 4, 191-200, April 2025


*Original Article*

# Design and Implementation of Photovoltaic Emulator for Testing of Photovoltaic Energy Conversion System

Krismadinata[1,2], Silvi Anggraini[2], Asnil[2], Rudi Mulya[2], Syafii[3], and Fahmi[4]

[1]*Centre for Energy and Power Electronics Research (CEPER), Universitas Negeri Padang, Indonesia.*
[2]*Department of Electrical Engineering, Universitas Negeri Padang, Indonesia,*
[3]*Department of Electrical Engineering, Universitas Andalas, Padang, Indonesia.*
[4]*Department of Electrical Engineering, Universitas Sumatera Utara, Medan, Indonesia.*

[1]*Corresponding Author : krisma@ft.unp.ac.id*

Received: 10 February 2025 Revised: 12 March 2025 Accepted: 13 April 2025 Published: 29 April 2025

***Abstract*** *- This paper discusses the design and assembly of PV emulators to employ in power converter testing on solar power plant systems. The design process starts with simulating the features of a Photovoltaic (PV) module based on the factors it has. The buck converter serves as a virtual PV module. These models are then simulated, tested, and built hardware for Photovoltaic Emulators (PVE). A cheap Arduino Uno microcontroller processes the activities of a PVE. The suggested PVE includes a Graphical User Interface (GUI) based on Matlab. The Proportional, Integral, Differential (PID) controller controls the current and output voltage of the buck converter to acquire the precision of the current and voltage settings of the converter buck, which is a function of the solar module's irradiation and temperature. The proposed PVE uses Solkar 36-Watt PV modules as a model. The experiment results show that the suggested PVE can be used as a PV module simulator in power converter testing at solar power plants and as a substitute for the real PV module.*

***Keywords*** *- PV module, PVE, Buck converter, PID controller, Matlab GUI*

## 1. Introduction

The high growth of solar panel energy is due to the benefits that solar panels have, such as lower operating costs, no moving parts, and an abundant amount of raw materials [1]. On the other hand, in real-time experiments, there are some drawbacks such as high initial costs, requiring a large area to install solar panels in series and parallel, time-consuming to connect solar panels [2], dependence on weather conditions and repeated testing to determine the MPPT algorithm [3].

Therefore, a laboratory testing tool that replicates the characteristics of solar panels without the limitations of environmental dependence is necessary. This requirement is addressed by implementing the PVE [4]. A significant distinction between PVE and actual PV modules is that PV modules directly convert solar irradiance into electricity, heavily relying on environmental factors, while PVEs artificially replicate these characteristics in controlled lab environments without dependence on external conditions. PV emulator technology has evolved significantly, ranging from basic emulators using simple DC-DC converters to advanced microcontroller-based systems. PVEs produce voltage-current (I-V) characteristics identical to real PV modules, unaffected by varying weather conditions, making them crucial tools in solar energy research.

Recent studies highlight the importance of precise control mechanisms such as fuzzy logic controllers and neural network algorithms to emulate PV characteristics accurately. Previous researchers have developed several studies regarding PVE technology. These include the development of a solar altitude emulator CO3208-1B board [5], an emulator based on a Switch Mode Power Supply (SMPS) [6], and implementations utilizing low-cost microcontrollers [7].

Other notable contributions involve the Typhoon Hardware-In-The-Loop (HIL) 402 emulator [8, 9], the modular E4360 Keysight [10], and various DC-DC converter topologies such as the buck converter [11], the two-switch non-inverting buck-boost DC/DC converter combined with a diode string [12], and a GaN-Based synchronous buck Converter [13].

Additionally, several studies have focused on PV cell modelling approaches, including the use of PV cell equivalent circuit models [14], partial shading investigations [15], and single diode models [16]. Advanced control and emulation methods have also been explored, such as Artificial Neural Networks combined with nonlinear backstepping controllers [17], adaptive time-stepping-based real-time EMT emulation [18], fuzzy state-feedback control [19], the resolution of

mathematical models for PV modules [20], and buck converters integrated with GUI [21].

Additionally, recent developments have emphasized the role of PID controllers as a reliable and cost-effective solution for regulating output in photovoltaic emulation. For instance, [22] demonstrated the integration of adaptive Maximum Power Point Tracking (MPPT) controllers with PID structures to improve emulator performance [23, 24]. Furthermore, [25] conducted a comparative analysis of MPPT algorithms, underlining the critical role of PID tuning for emulator stability.

This paper presents a prototype photovoltaic emulator, highlighting advancements in solar panel emulation for more efficient and regulated testing. The novelty of this research lies in integrating a low-cost Arduino-based controller with a MATLAB GUI, accurately emulating PV characteristics. Beginning with rigorous simulations of PV module features influenced by temperature and irradiance, this study significantly improves existing designs by clearly defining operational conditions and conducting extensive comparative analyses with real PV modules. A buck converter controlled by a PID controller acts as a virtual PV panel, producing output currents and voltages closely resembling real solar cell behavior across varying load conditions, all monitored through a user-friendly MATLAB interface.

## 2. Photovoltaic Modelling

A PV module is a PV generating system's essential power conversion unit. The performance of the PV module is influenced by the sun irradiance and the temperature of the solar cells. Due to the nonlinear nature of PV modules, it is essential to create a model for their design and simulation to implement MPPT for photovoltaic energy conversion systems [26]. There are a number of options to represent the properties of PV cells. The methodologies include linearization, numerical methods, analytical approaches, artificial intelligence methods, and their Thevenin counterparts [27-31]. A single diode equivalent circuit model can be implemented as a PV cells model (see Figure 1); the solar cell equivalent circuit has photovoltaic current, diode, series resistance ($R_s$) and parallel resistance ($R_{sh}$).

When sunlight strikes a solar cell directly, the current emitted by sunlight is called photovoltaic current or photocurrent. ($I_{pv}$). These currents change linearly with radiation intensity and are influenced by temperature. The series resistance (Rs) and parallel resistance ($R_{sh}$) of the circuit represents the resistance in series and parallel modes of the cell. In general, the $R_{sh}$ rating is higher than the $R_s$ rating. Equation (1) explains the principle of the solar cell equivalent circuit. The value of the solar cell current ($I_{pv}$) is the result of subtracting the current Iph, the diode current ($I_D$) and shunt current ($I_{rsh}$), which can be described as follows [32-35]:

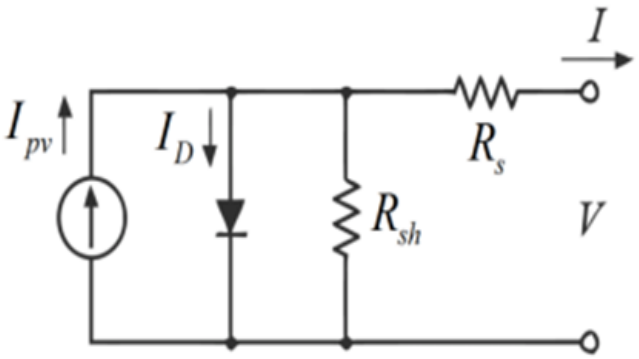


**Fig. 1 Equivalent circuit**

$$I_{pv} = I_{ph} - I_D - I_{rsh} \quad (1)$$

It also can be written as:

$$I_{pv} = N_p I_{ph} - N_s I_s \left( exp \frac{q(V_{pv}+I_{pv}R_s)}{N_s n K T_c} - 1 \right) - \frac{(V_{pv}+I_{pv}r_s)}{R_{sh}} \quad (2)$$

Where:

| | | |
|---|---|---|
| $I_s$ | = | photovoltaic saturation current |
| q | = | electron = $1.6 \times 10^{-19}$ C |
| $V_{pv}$ | = | voltage |
| $T_c$ | = | cell temperature |
| $R_s$ | = | series resistance |
| $R_{sh}$ | = | shunt resistance |
| n | = | ideal factor |
| k | = | Boltzmann's constant = $1.38 \times 10^{-23}$ J/K |
| $N_s$ | = | number of series solar cells |
| $N_p$ | = | number of parallel solar cells |

In the Equations (1) and (2), there are five unstated parameters. The five parameters include photovoltaic current ($I_{ph}$), solar cell saturation current ($I_s$), parallel resistance ($I_{rsh}$), series resistance ($I_s$), and diode ideal factor (n). Here are the equations for determining the current ($I_{ph}$) and current ($I_s$) for modeling solar cells:

- Photovoltaic current

$$I_{ph} = \left[ I_{sc} + K_i (T_c - T_{ref}) \right] \frac{\beta}{\beta_{ref}} \quad (3)$$

- Photovoltaic saturation current

$$I_s = I_{rs} \left[ \frac{T_c}{T_{ref}} \right]^3 exp \left[ \frac{qE_g}{nk} \left\{ \frac{1}{T_{ref}} - \frac{1}{T_c} \right\} \right] \quad (4)$$

- Dark saturation current

$$I_{rs} = I_{sc-ref} / \left[ exp(qV_{oc-ref} / NsknT_{ref}) - 1 \right] \quad (5)$$

- Series resistance

$$R_s = \frac{\frac{N_s n K T_c}{q} ln\left(1-\frac{I_m}{I_{sc}}\right)+V_{oc}-V_m}{I_m} \quad (6)$$

- Ideal factor

$$R_{sh} = \frac{0.5V_{oc}-V_{sc}}{I_{sc}-I_x} \quad (7)$$

The 37Wp PV Panel (Solkar-36) is employed and modelled without considering the partial shading effect of the PV panel. The photovoltaic emulator circuit comprises a DC source and a DC-DC buck converter. The size of the capacitor and inductor for filter design in buck converter can be determined with Equations (8) to (11).

The critical value of inductance to operate the converter in continuous conduction mode is given by:

$$\Delta I_L = \frac{V_{in}D(1-D)}{fL} \quad (8)$$

$$L = \frac{V_{in}D(1-D)}{f\Delta I_L} \quad (9)$$

The size of capacitance depends on peak-to-peak ripple voltage and is given by:

$$\Delta V = \frac{V_{in}D(1-D)}{8LCf^2} \quad (10)$$

$$C = \frac{V_{in}D(1-D)}{8L\Delta Vf^2} \quad (11)$$

## 3. Design and Implementation

The PVE was designed to accurately simulate a Solkar 36-Watt PV module under strictly defined conditions, specifically irradiance levels of 500, 700, and 1000 W/m² and temperatures ranging from 30°C to 50°C in increments of 10°C. A buck converter, functioning as a virtual PV panel, was precisely controlled using a low-cost Arduino Uno microcontroller integrated with a PID controller. The simulated PV characteristics were translated into a tangible hardware setup, including necessary control circuits and interfaces, as depicted in Figure 2.

In Figure 2, the microcontroller utilizes embedded mathematical equations and PID algorithms. By entering specific irradiance, temperature, and real-time feedback from the buck converter's output current and voltage, a reference current is computed. The PID controller adjusts the output current from the buck converter to align it precisely with the reference, ensuring realistic behavior akin to an actual PV module. The PWM signals generated by the Arduino facilitate precise control of the buck converter switches, dynamically matching PV characteristics as load conditions change. Clear testing conditions were established to thoroughly evaluate the emulator's accuracy against an actual PV module. The PVE underwent rigorous experiments comparing its outputs under various defined irradiance and temperature scenarios with those from a real Solkar PV module. The tests systematically varied the parameters and included comparative analysis at incremental temperature and irradiance levels. Monitoring was performed in real-time using a MATLAB Graphical User Interface (GUI) along with an LCD display that continuously provided current and voltage readings.

Figure 3 presents the detailed block diagram of the emulator's configuration, clearly outlining each component and their interactions. Figure 4 shows the detailed flowchart used during the software development phase, ensuring logical coherence and alignment of the system operations with established simulation and testing parameters.

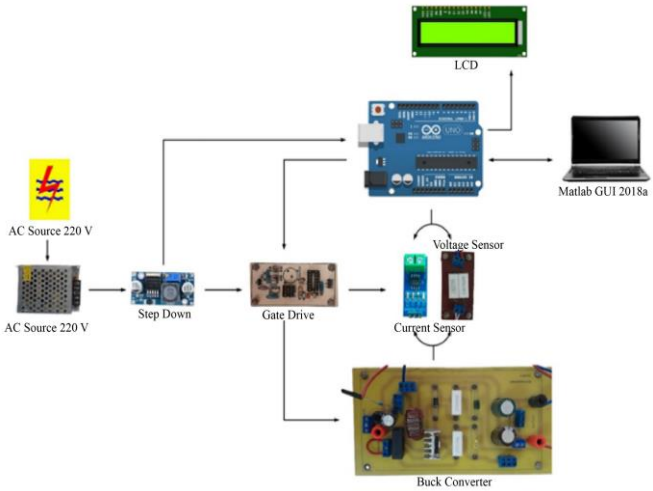


**Fig. 2 The PVE system configuration**

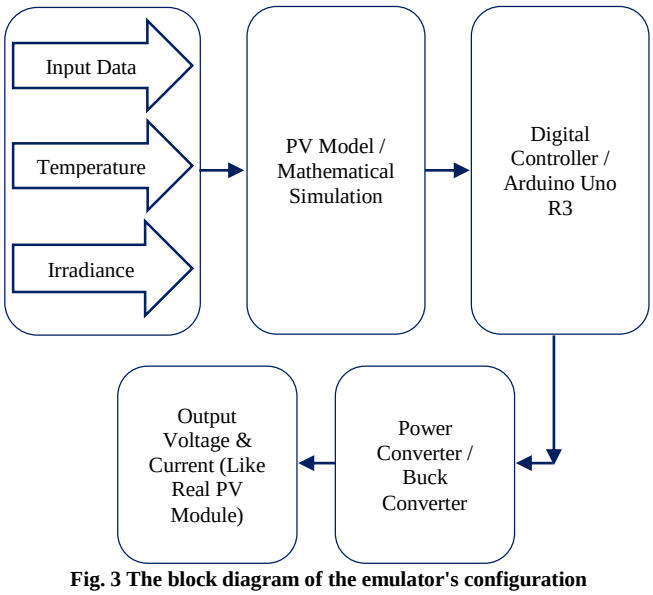


**Fig. 3 The block diagram of the emulator's configuration**

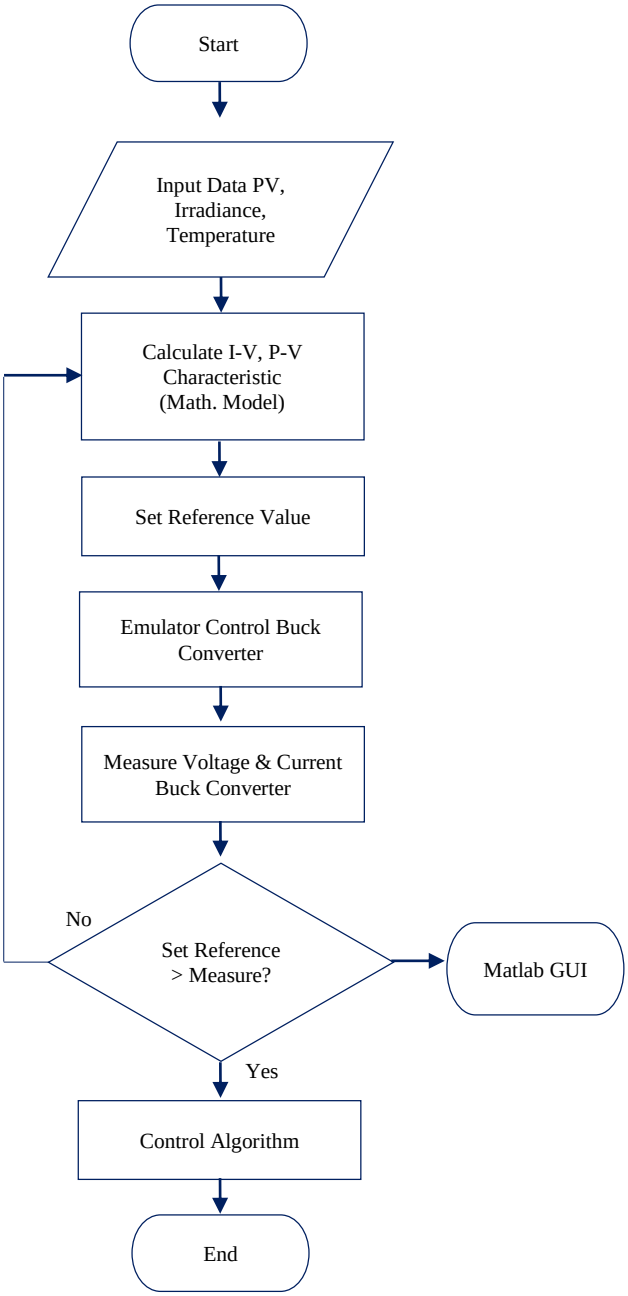


**Fig. 4 Flowchart of the PVE**

## 4. Results and Discussion

### *4.1. Simulating Results*

To thoroughly evaluate the performance and accuracy of the proposed PVE, a structured set of testing parameters was established, simulating realistic operating conditions of photovoltaic systems. The primary variables tested included irradiance levels, cell temperature, and load resistance. Irradiance was varied across three levels—500 W/m², 700 W/m², and 1000 W/m² representing low, moderate, and standard solar radiation intensities, respectively. These levels allowed for assessment under both overcast and clear-sky conditions in accordance with industry standards. Likewise, the temperature was adjusted in increments of 10°C, ranging from 30°C to 50°C, to replicate the typical operational thermal conditions of solar modules in real-world scenarios. Load resistance was also varied extensively, from 1 Ω to 320 Ω, to examine the PVE's behavior under different electrical demands and capture the resulting *I-V* and *P-V* characteristics across a wide operational range.

In addition to these variations, testing under Standard Test Conditions (STC)-which include an irradiance of 1000 W/m² and a cell temperature of 25°C-was conducted to benchmark the emulator's performance against the actual Solkar 36-Watt PV module specifications. All experiments were performed in a controlled laboratory environment using programmable power supplies and heating elements to simulate the desired irradiance and temperature values. This ensured consistent and repeatable test results without external environmental interference. Real-time monitoring and data acquisition was facilitated through a MATLAB-based GUI, providing both graphical and numerical voltage, current, and power outputs.

The system also included an LCD display for on-device monitoring and allowed data export for further analysis. This rigorous testing methodology ensured a comprehensive validation of the PVE's capability to replicate real PV module behavior accurately under dynamic operating conditions. The PV module employed to reference is shown in Table 1.

**Table 1. Parameter of Solkar 36 Watt module at STC**

| No | Parameter | Rate |
|---|---|---|
| 1 | Maximum Power ($P_m$) | 37.08 W |
| 2 | Voltage at Maximum Power ($V_m$) | 16.56 V |
| 3 | Current at Maximum Power ($I_m$) | 2.25 A |
| 4 | Open Circuit Voltage ($V_{oc}$) | 21.24 V |
| 5 | Short Circuit Current ($I_{sc}$) | 2.55 A |
| 6 | Number of Series Cells ($N_s$) | 36 |
| 7 | Series Resistance ($R_s$) | 0.1 |
| 8 | Parallel Resistance ($R_{sh}$) | 10620 |
| 9 | Ideal Factor (n) | 1.6 |

After the system is designed, it is then modeled into mathematical form. The block diagram of the integrated system with the modified PV model attached is displayed in Figure 5. The PVE design includes several components: an Arduino Uno microcontroller, gate drive circuit, buck converter circuit, voltage sensor, current sensor, and load. Each component has its own role and is interconnected with other components.

Specifying the PID constants is an important step because it affects the performance of a system. This method identifies the plant model from the input-output test data. PID controller modeling is done with the PID controller block in Simulink (Figure 6). Furthermore, the *P, I, and D* values are obtained and can be adjusted to achieve a more favorable one.

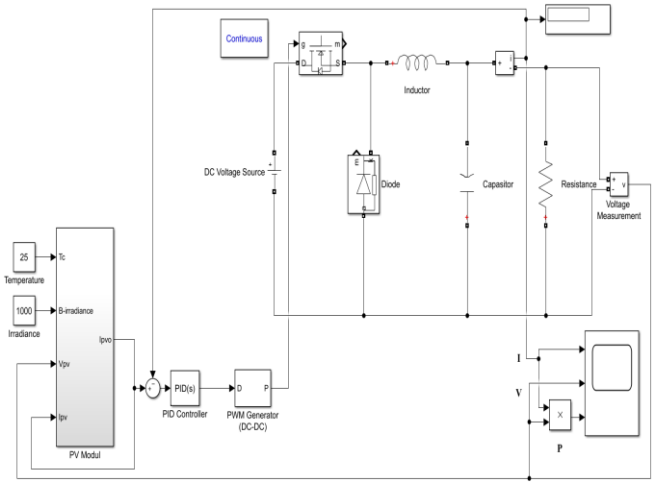


**Fig. 5 Photovoltaic emulator modeling**

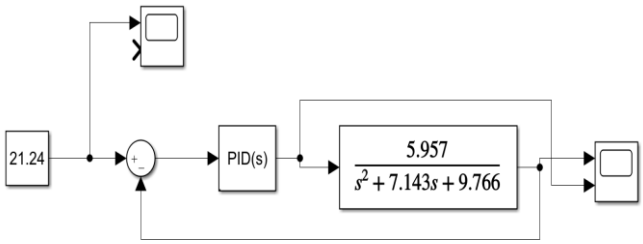


**Fig. 6 PID controller in Simulink Matlab**

The simulation illustrated in Figure 7 shows that the electrical current generated by a solar panel varies with voltage across different irradiance levels (1000 W/m², 700 W/m², and 500 W/m²). At higher irradiance levels, the current produced is greater, indicating that the solar panel can generate more current under stronger lighting conditions. Figure 8 shows the *I-V* curve simulation of a solar panel at different temperatures: 30°C, 40°C, and 50°C. The curves indicate that higher temperatures lead to decreased solar panel performance, with lower current generated at higher temperatures, reducing the panel's efficiency in producing electricity.

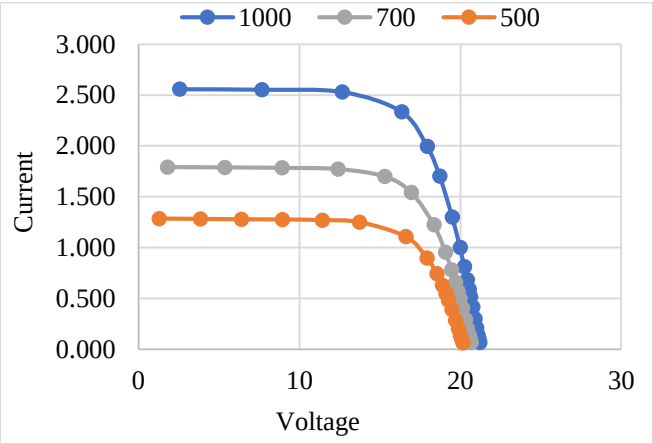


**Fig. 7 Curves at varying irradiances**

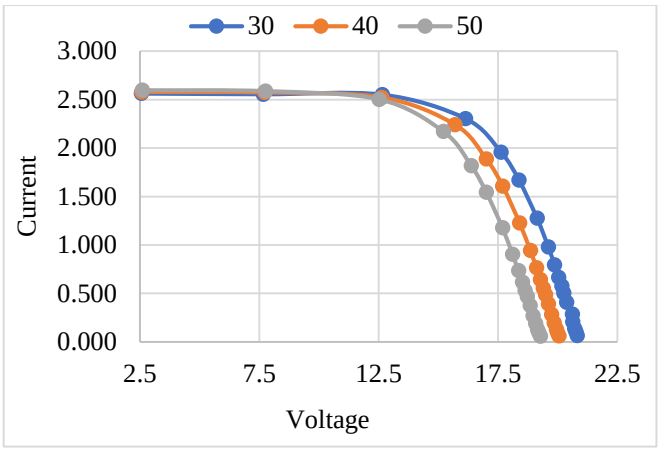


**Fig. 8 I-V curve of varying temperatures**

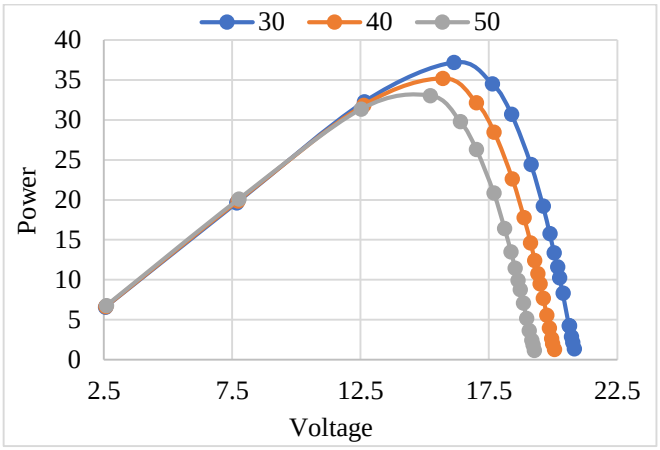


**Fig. 9 P-V curve on varying irradiances**

The simulation results in Figure 9 shows that the higher the irradiance value, the greater the maximum power generated, with the voltage at the Maximum Power Point also tending to be higher.

This indicates solar panels will produce more power and operate more efficiently under stronger lighting conditions.

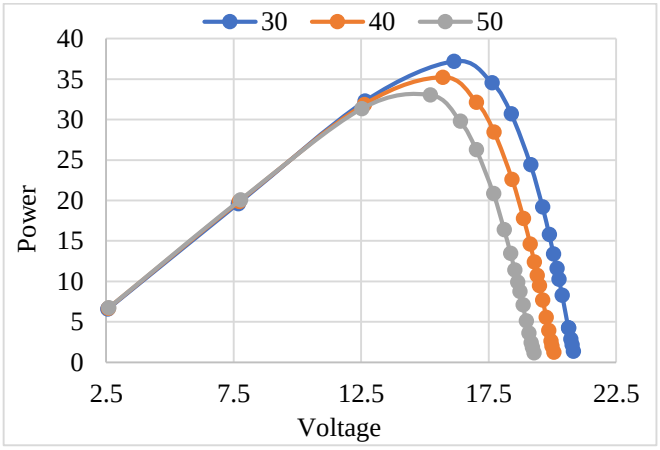


**Fig. 10 P-V curves of varying temperatures**

The P-V curve in Figure 10 shows that when the temperature rises from 30°C to 50°C, the maximum power output falls, as does the voltage at the MPP. This suggests solar modules perform better at lower temperatures, while higher temperatures diminish voltage and overall power output.

### *4.2. Experimental Buck Converter*

Experimental tests are conducted to evaluate the performance of the solar simulator and validate its ability to replicate solar irradiance accurately.

The buck converter output voltage response without a controller is shown in Figure 11. The output voltage is achieved without overshoot and fast rise time, but the output voltage cannot be controlled. The PID controller is employed to regulate it.

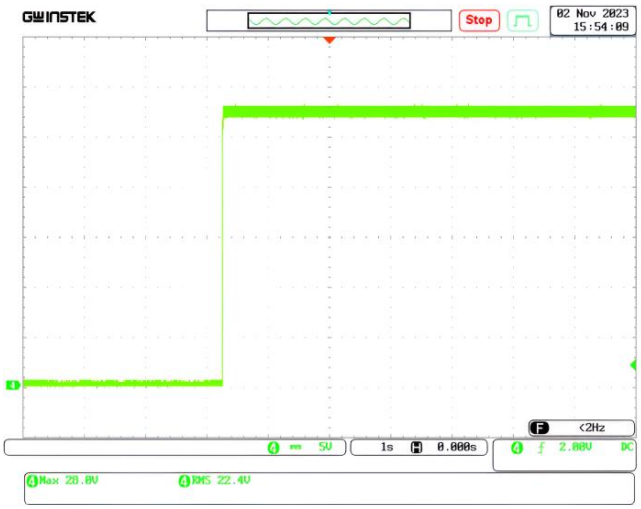


**Fig. 11 The buck converter without controller**

The output voltage of the buck converter employing the PID controller is shown in Figure 12.

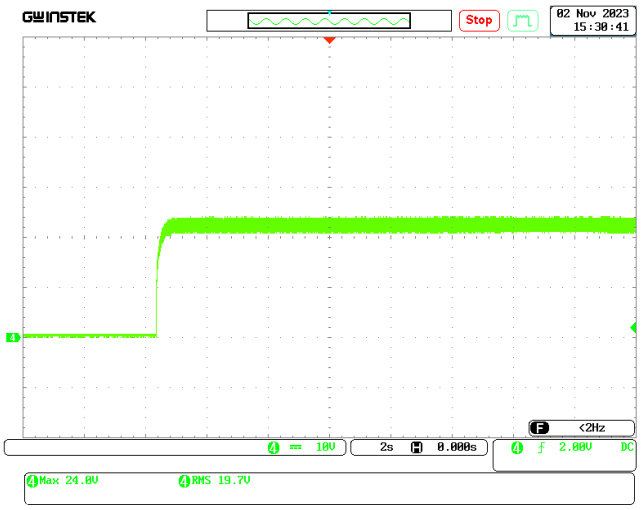


**Fig. 12 Output voltage with PID controller**

The PID controller's automated tuning yielded the following results: P = 48.58, I = 29.92 and D = 0.55. The graph in Figure 8 represents the output voltage response of the buck converter, with a set point of 21.24 V. The rise time on the PID response graph is marginally slower compared to the buck converter without the controller. Figure 13 can be the output voltage of the buck converter with varying input and employing a PID controller. The voltage can be regulated.

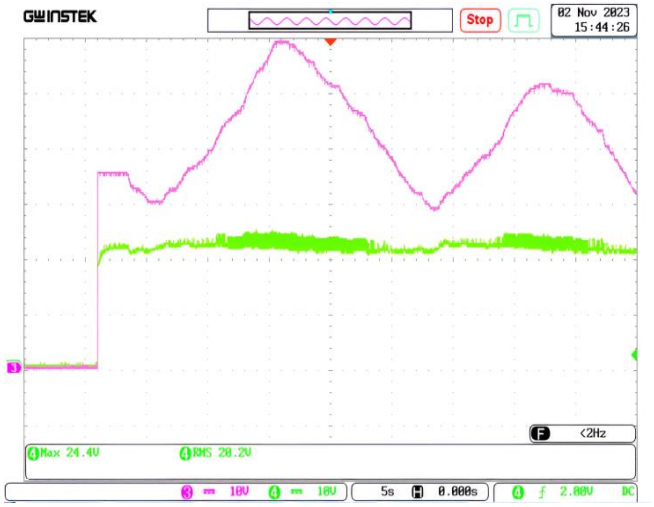


**Fig. 13 Output voltage varying input**

### *4.3. Photovoltaic Emulator Testing*

To verify the accuracy and performance of the proposed PVE, comprehensive experimental testing was conducted under various environmental conditions. The results were directly compared to the characteristics of the real Solkar 36-Watt PV module under identical conditions. The parameters varied included irradiance (500 W/m², 700 W/m², 1000 W/m²), temperature (30°C to 50°C in 10°C increments), and load resistance (1 Ω to 320 Ω). Figures 14–17 illustrate the emulator's current-voltage (I-V) and power-voltage (P-V) characteristics under these varying conditions. These were systematically compared to the known standard characteristics of the reference Solkar module listed in Table 1.

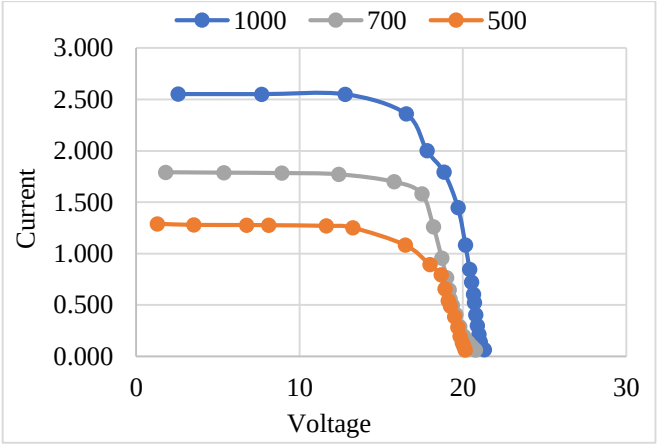


**Fig. 14 I-V curve of PVE under varying radiation**

Figure 14 presents the current-voltage (I-V) characteristics of the PVE under various radiation levels. The PVE closely mirrors the Solkar module behavior, where increasing irradiance from 500 W/m² to 1000 W/m² increased the short-circuit current from ~1.3 A to ~2.55 A. Voltage remained relatively stable across irradiance changes, matching the Solkar module's Voc of ~21.24 V. Figure 15 illustrates the I-V characteristics of the device under test varying temperature conditions. The emulator accurately reflects the temperature dependency of Voc, showing a decrease from ~21.2 V at 30°C to ~20.2 V at 50°C, closely matching theoretical expectations. The current remained relatively unchanged, indicating the emulator's ability to preserve the temperature-independent performance of $I_{sc}$.

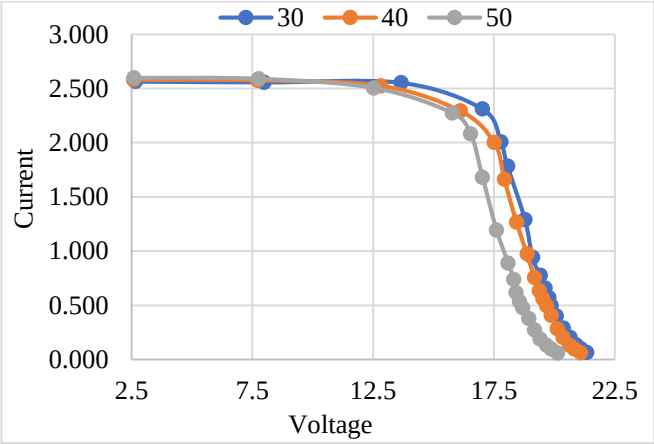


**Fig. 15 I-V curve of PVE under varying temperature**

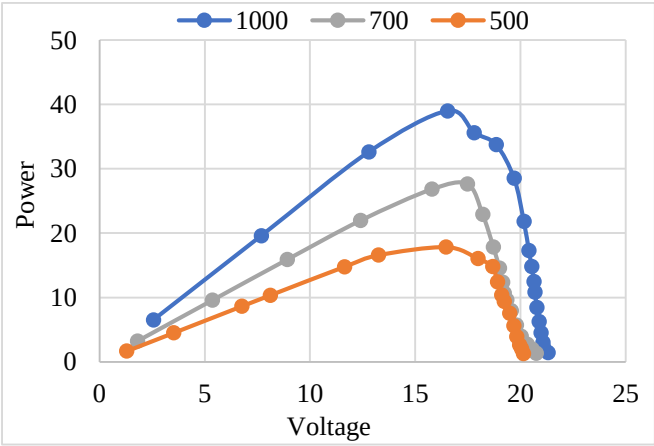


**Fig. 16 P-V curve of PVE under varying radiation**

Power-Voltage (P-V) characteristics of the PVE are depicted in Figure 16, which shows how these characteristics change under different radiation situations. Power output increased with irradiance, peaking at approximately 37 W at 1000 W/m², consistent with Solkar's rated maximum power ($P_m$).

The voltage at the maximum power point ($V_{mp}$) also increased, ranging from ~15 V (500 W/m²) to ~16.5 V (1000 W/m²), in alignment with standard PV module behavior.

The Power-Voltage (P-V) characteristics of the PVE under varying temperature environments are presented in Figure 17. A clear drop in maximum power output was observed with rising temperature: from ~37 W at 30°C to ~34 W at 50°C-a ~9% drop, matching typical de-rating factors (~0.4%/°C). The voltage at maximum power ($V_{mp}$) dropped consistently by ~0.25 V per 10°C, confirming realistic thermal modeling in the emulator.

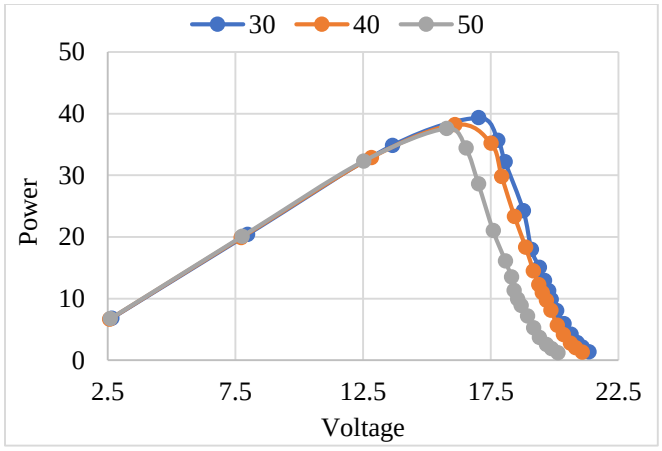


**Fig. 17 P-V curves of PVE under varying temperatures**

Table 2 presents a detailed quantitative comparison of the PVE and Solkar modules under Standard Test Conditions (STC).

As depicted in Figure 18, a GUI is employed to monitor and display the measured parameters from the PVE. The interface presents data in graphical and numerical formats, including I-V and P-V characteristics. Additionally, the application facilitates the direct export of data to Excel format for further analysis.

**Table 2. Quantitative comparison between PVE and Solkar Module Under STC**

| Parameter | Solkar 6W (STC) | PVE Output (STC) | Deviation (%) |
|---|---|---|---|
| Max Power ($P_m$) | 37.08 W | 36.92 W | -0.43% |
| Voltage at Max Power ($V_m$) | 16.56 V | 16.40 V | -0.96% |
| Current at Max Power ($I_m$) | 2.25 A | 2.27 A | +0.89% |
| Open Circuit Voltage ($V_{oc}$) | 21.24 V | 21.20 V | -0.19% |
| Short Circuit Current ($I_{sc}$) | 2.55 A | 2.53 A | -0.78% |

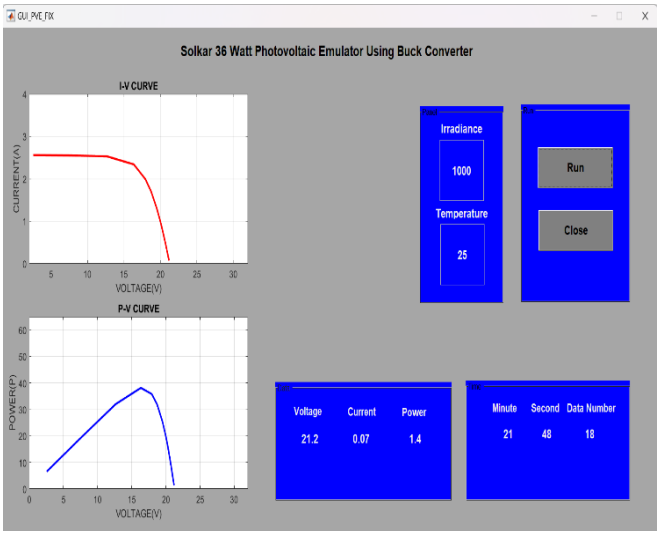


**Fig. 18 Photovoltaic emulator monitoring**

## 5. Conclusion

The investigation into the PVE designed to simulate solar panel settings in a laboratory environment has shown satisfactory results. The study tackled the constraints of traditional solar panel testing, which necessitates particular climatic conditions, by concentrating on a maximum power point tracking control algorithm MPPT and an adaptive power stage. The PVE, driven by an Arduino Uno and operated via a MATLAB GUI, accurately duplicates the characteristics of a Solkar 36-Watt PV module utilizing a buck converter and PID controller. This facilitates accurate control of irradiance and temperature parameters, rendering the PVE a dependable instrument for testing solar power plant systems. The results validate that the emulator not only replaces actual PV modules but also improves the evaluation of power converters, illustrating its viability as a practical and safer option in solar energy research.

## Acknowledgments

The authors sincerely thank the Ministry of Education, Culture, Research, and Technology of the Republic of Indonesia and the Institute for Research and Community Services at Universitas Negeri Padang for their valuable support through the Applied Research Scheme. This work was funded under Project No. 1753/UN35.13/LT/2022.

## References

[1] Marcos García-López, Borja Montano, and Joaquín Melgarejo, "Household Energy Consumption and the Financial Feasibility of Self-Consumption through Photovoltaic Panels in Spain," *Energy Efficiency*, vol. 16, no. 6, pp. 1-17, 2023. [CrossRef] [Google Scholar] [Publisher Link]

[2] Ahmed M.T. Ibraheem Al-Naib, and Majeed Ismail Mohammed, "IoT-Based Real Time Data Acquisition of PV Panel," *IEEE International Conference on Engineering, Science and Advanced Technology*, Mosul, Iraq, pp. 169-173, 2023. [CrossRef] [Google Scholar] [Publisher Link]

[3] Asier del Rio et al., "Particle Swarm Optimization-Based Control for Maximum Power Point Tracking Implemented in a Real Time Photovoltaic System," *Information*, vol. 14, no. 10, pp. 1-16, 2023. [CrossRef] [Google Scholar] [Publisher Link]

[4] Kemal Bilen, and İsmail Erdoğan, "Effects of Cooling on Performance of Photovoltaic/Thermal (PV/T) Solar Panels: A Comprehensive Review," *Solar Energy*, vol. 262, 2023. [CrossRef] [Google Scholar] [Publisher Link]

[5] Ahmed Hussain Elmetwaly et al., "Modeling, Simulation, and Experimental Validation of a Novel MPPT for Hybrid Renewable Sources Integrated with UPQC: An Application of Jellyfish Search Optimizer," *Sustainability*, vol. 15, no. 6, pp. 1-30, 2023. [CrossRef] [Google Scholar] [Publisher Link]

[6] Mohammed Chaker et al., "Development of a PV Emulator using SMPS Converter and a Model Selection Mechanism for Characteristic Generation," *Solar Energy*, vol. 239, pp. 117-128, 2022. [CrossRef] [Google Scholar] [Publisher Link]

[7] Abdelkadir Boucharef et al., "Solar Module Emulator Based on a Low-Cost Microcontroller," *Measurement*, vol. 187, 2022. [CrossRef] [Google Scholar] [Publisher Link]

[8] A. Nazar Ali et al., "Design and Development of Realistic PV Emulator Adaptable to the Maximum Power Point Tracking Algorithm and Battery Charging Controller," *Solar Energy*, vol. 220, pp. 473-490, 2021. [CrossRef] [Google Scholar] [Publisher Link]

[9] Javed Ahmad et al., "Performance Analysis and Hardware-in-the-Loop (HIL) Validation of Single Switch High Voltage Gain DC-DC Converters for MPP Tracking in Solar PV System," *IEEE Access*, vol. 9, pp. 48811-48830, 2021. [CrossRef] [Google Scholar] [Publisher Link]

[10] Nabil A. Ahmed, Salahuddin Abdul Rahman, and Bader N. Alajmi, "Optimal Controller Tuning for P&O Maximum Power Point Tracking of PV Systems Using Genetic and Cuckoo Search Algorithms," *International Transactions on Electrical Energy Systems*, vol. 31, no. 10, 2020. [CrossRef] [Google Scholar] [Publisher Link]

[11] Cagfer Yanarates, Yidong Wang, and Zhongfu Zhou, "Unity Proportional Gain Resonant and Gain Scheduled Proportional (PR-P) Controller-Based Variable Perturbation Size Real-Time Adaptive Perturb and Observe (PO) MPPT Algorithm for PV Systems," *IEEE Access*, vol. 9, pp. 138468-138482, 2021. [CrossRef] [Google Scholar] [Publisher Link]

[12] Habes Ali Khawaldeh et al., "Efficiency Improvement Scheme for PV Emulator Based on a Physical Equivalent PV-Cell Model," *IEEE Access*, vol. 9, pp. 83929-83939, 2021. [CrossRef] [Google Scholar] [Publisher Link]

[13] Chao-Tsung Ma et al., "Design and Implementation of a Flexible Photovoltaic Emulator Using a Gan-Based Synchronous Buck Converter," *Micromachines*, vol. 12, no. 12, pp. 1-16, 2021. [CrossRef] [Google Scholar] [Publisher Link]

[14] Habes A. Khawaldeh et al., "Fast Photovoltaic Emulator Based on PV-Cell Equivalent Circuit Model," *IEEE 12th Energy Conversion Congress and Exposition - Asia*, Singapore, pp. 2121-2126, 2021. [CrossRef] [Google Scholar] [Publisher Link]

[15] Dan Craciunescu, and Laurentiu Fara, "Investigation of the Partial Shading Effect of Photovoltaic Panels and Optimization of their Performance Based on High-Efficiency FLC Algorithm," *Energies*, vol. 16, no. 3, pp. 1-28, 2023. [CrossRef] [Google Scholar] [Publisher Link]

[16] S. Senthilkumar et al., "Analysis of Single-Diode PV Model and Optimized MPPT Model for Different Environmental Conditions," *International Transactions on Electrical Energy Systems*, vol. 2022, no. 1, pp. 1-17, 2022. [CrossRef] [Google Scholar] [Publisher Link]

[17] Ambe Harrison, and Njimboh Henry Alombah, "A New Piecewise Segmentation Based Solar Photovoltaic Emulator Using Artificial Neural Networks and a Nonlinear Backstepping Controller," *Applied Solar Energy*, vol. 59, no. 3, pp. 283-304, 2023. [CrossRef] [Google Scholar] [Publisher Link]

[18] Venkata Dinavahi, and Ning Lin, *Adaptive Time-Stepping Based Real-Time EMT Emulation*, Real-Time Electromagnetic Transient Simulation of AC-DC Network, Wiley-IEEE Press, pp. 217-252, 2021. [CrossRef] [Google Scholar] [Publisher Link]

[19] Karima El Hammoumi, Redouane Chaibi, and Rachid El Bachtiri, "Fuzzy State-Feedback Control for MPPT of Photovoltaic Energy with Storage System," *International Journal of Innovative Computing, Information and Control*, vol. 18, no. 1, pp. 253-270, 2022. [CrossRef] [Google Scholar] [Publisher Link]

[20] Mohammed Rasheed et al., "Mathematical Models for Resolving the Nonlinear Formula for Solar Cell," *Indonesian Journal of Electrical Engineering and Computer Science*, vol. 33, no. 1, pp. 653-660, 2024. [CrossRef] [Publisher Link]

[21] Benjamin Dean et al., "A Graphical User Interface Platform to Support Power Electronic Converters and Integrated Systems," *IEEE Power and Energy Society Innovative Smart Grid Technologies Conference*, Washington, DC, USA, pp. 1-5, 2024. [CrossRef] [Google Scholar] [Publisher Link]

[22] Razman Ayop et al., "Photovoltaic Emulator Using Error Adjustment Fuzzy Logic Proportional-Integral Controller," *International Journal of Power Electronics and Drive Systems*, vol. 13, no. 2, pp. 1111-1118, 2022. [CrossRef] [Google Scholar] [Publisher Link]

[23] Wenqiang Zhu et al., "A Novel Simplified Buck Power System Control Algorithm: Application to the Emulation of Photovoltaic Solar Panels," *Computers and Electrical Engineering*, vol. 116, 2024. [CrossRef] [Google Scholar] [Publisher Link]

[24] Saibal Manna et al., "Design and Implementation of a New Adaptive MPPT Controller for Solar PV Systems," *Energy Reports*, vol. 9, pp. 1818-1829, 2023. [CrossRef] [Google Scholar] [Publisher Link]

[25] Zouhaira Ben Mahmoud, Intissar Moussa, and Adel Khedher, "Implementation of MPPT Algorithms to a Developed Photovoltaic Emulator: Study and Comparative Analysis," *IEEE 11th International Conference on Systems and Control*, Sousse, Tunisia, pp. 719-724, 2023. [CrossRef] [Google Scholar] [Publisher Link]

[26] Bidjagare Akiza, Edjadessamam Akoro, and Dam-Bé L. Douti, "Design and Simulation of an MPPT Charge Controller for a PV Application," *TH Wildau Engineering and Natural Sciences Proceedings*, Kara, UK, vol. 1, pp. 257-261, 2021. [CrossRef] [Google Scholar] [Publisher Link]

[27] Abdulwahab A.Q. Hasan, Ammar Ahmed Alkahtani, and Nowshad Amin, "Modeling and Performance Evaluation of Solar Cells Using I-V Curve Analysis," *Proceedings of the 2nd International Conference on Emerging Technologies and Intelligent Systems*, pp. 643-650, 2023. [CrossRef] [Google Scholar] [Publisher Link]

[28] Haonan Fang et al., "A Linearization Based Model Equivalent Method for Distributed Photovoltaic Generation Clusters," *IEEE 6th Conference on Energy Internet and Energy System Integration (EI2)*, Chengdu, China, pp. 1-5, 2022. [CrossRef] [Google Scholar] [Publisher Link]

[29] Ahmed Shawki Jaber et al., "Comparesion the Electrical Parameters of Photovoltaic Cell Using Numerical Methods," *EUREKA: Physics and Engineering*, vol. 4, no. 4, pp. 29-39, 2023. [CrossRef] [Google Scholar] [Publisher Link]

[30] Lsmail Hburi, Hasan Fahad, and Ali Assad, "Powerful Maximum Power Point Tracking for PV Systems: An Artificial Intelligence Paradigm," *IEEE Iraqi International Conference on Communication and Information Technologies*, Basrah, Iraq, pp. 280-286, 2022. [CrossRef] [Google Scholar] [Publisher Link]

[31] Suleyman Adak et al., "Thevenin Equivalent of Solar PV Cell Model and Maximum Power Transfer," *IEEE International Conference on Electrical, Communication, and Computer Engineering*, Kuala Lumpur, Malaysia, pp. 1-5, 2021. [CrossRef] [Google Scholar] [Publisher Link]

[32] Victor Daldegan Paduani et al., "A Unified Power-Setpoint Tracking Algorithm for Utility-Scale PV Systems with Power Reserves and Fast Frequency Response Capabilities," *IEEE Transactions on Sustainable Energy*, vol. 13, no. 1, pp. 479-490, 2022. [CrossRef] [Google Scholar] [Publisher Link]

[33] Mahendiran Vellingiri et al., "Non-Linear Analysis of Novel Equivalent Circuits of Single-Diode Solar Cell Models with Voltage-Dependent Resistance," *Fractal and Fractional*, vol. 7, no. 1, pp. 1-26, 2023. [CrossRef] [Google Scholar] [Publisher Link]

[34] Maria Amaidi, Lassaad Zaaraoui, and Ali Mansouri, "Enhanced Method for Estimating Unknown Parameters in Single Diode Model for Solar Photovoltaic Cells," *Malaysian Journal of Fundamental and Applied Sciences*, vol. 20, no. 3, pp. 648-660, 2024. [CrossRef] [Google Scholar] [Publisher Link]

[35] Imade Choulli et al., "A Novel Hybrid Analytical/Iterative Method to Extract the Single-Diode Model's Parameters Using Lambert's W-Function," *Energy Conversion and Management: X*, vol. 18, 2023. [CrossRef] [Google Scholar] [Publisher Link]